Direct Kinetic Study of the Reaction of $Cl_2^{\bullet-}$ Radical Anions with Ethanol at the Air−Water Interface

R. S. Strekowski,[†] R. Remorov,[†,‡] and Ch. George*[,†]

Laboratoire d'Application de la Chimie à l'Environnement (UCBL-CNRS), 43 boulevard du 11 Novembre 1918, F-69622 Villeurbanne, France, and Institute of Chemical Physics, Russian Academy of Science, 4 Kosygin Street, Moscow 117977, Russia

Received: May 24, 2002; In Final Form: November 26, 2002

This work focuses on the development and application of the UV diffuse reflectance−laser flash photolysis technique to directly study the kinetics of reactions occurring at the gas−liquid-phase boundary. The reaction of $Cl_2^{\bullet-}$ radical anion with ethanol was chosen to directly "probe" the reaction kinetics at the air−water surface. The reaction rates at the surface are shown to be more rapid than in the bulk liquid. Direct kinetic evidence is provided that the reaction of $Cl_2^{\bullet-}$ radical anion with ethanol is at least 2 times faster at the surface than in the bulk. The rate coefficient for the surface reaction $Cl_2^{\bullet-}$ + ethanol is found to be $(4.45 \pm 0.80) \times 10^5$ M^{-1} s^{-1}. For comparison, the rate coefficient for the reaction of $Cl_2^{\bullet-}$ with ethanol in the aqueous phase is found to be $(1.77 \pm 0.34) \times 10^5$ M^{-1} s^{-1}. The uncertainties in the above expressions are 2σ and represent precision only. The effective rate coefficient for the aqueous-phase reaction $Cl_2^{\bullet-}$ + ethanol is found to be consistent with what has been reported. Therefore, the chemistry at the interface differs from that of the gas phase or liquid phase. The nature of interfacial reactions and their atmospheric implications are discussed.

Introduction

Heterogeneous gas−liquid interactions have been shown to play an important role in atmospheric processes such as the destruction of the stratospheric ozone layer, nonozone compliance in urban or rural environments, acid rain, global warming, the production of photochemical smog in urban−rural settings, and the formation of cloud condensation nuclei.[1−3] The laws governing the kinetics of heterogeneous reactions are generally very complex. Typically, the gas uptake into a liquid is governed by several processes, including gas-phase diffusion, mass accommodation, solubility, and liquid-phase chemical reaction.[4−6] For many soluble and less soluble atmospheric species the uptake of gas by water surfaces is measured to be entirely consistent with calculations based on the bulk aqueous chemistry of the species.[4,7,8] However, there has been increased recognition and a growing body of field[9] and laboratory data[9,10] that suggest that processes at the air−water interface can play a key role in the uptake and reactions of atmospheric gases with liquid droplets. That is, more efficient reactions may occur at the air−water interface itself. Atmospheric species may react at the interface without actually being taken up into the bulk of the solution.[5] For instance, field observations at a North American coastline suggest that an unrecognized chlorine source must exist which cannot be described by a known sequence of gas-phase and heterogeneous reactions.[9] Also, the uptake of gaseous SO_2 into a liquid cannot be explained by liquid-phase chemistry alone.[5,10−12] It has been shown that the atmospheric oxidation of SO_2(g) proceeds via the formation of a bound complex at the air−water interface.[5,11,12] Similarly, the atmospheric uptakes of acetaldehyde[4,13] and glyoxal[14] cannot be described solely by liquid-phase chemistry and are best explained in terms of enhanced reactivity at the gas−liquid interface. In another example, the uptake of Cl_2(g) and Br_2(g) by NaBr and NaI solutions cannot be explained with a simple aqueous-phase reaction mechanism and is best described if an additional channel at the gas−liquid interface participates in the reaction.[6,15,16] Moreover, George and co-workers observed that the uptake of gaseous BrCl[17] and $ClNO_2$[18] on NaI solutions was driven by bulk-phase chemistry but an additional surface reaction channel was found. Finlayson-Pitts and co-workers report that Cl_2(g) is produced when deliquesced sea salt particles are irradiated using 254 nm radiation in the presence of O_3.[10] The obtained experimental results are only explained in terms of ion-enhanced interactions with gases at aqueous interfaces.[10]

Clearly, the reactions occurring at the air−water interface are of great potential importance in the field of atmospheric sciences. Although the kinetics and dynamics of many of the gas- and liquid-phase reactions are more or less well understood, the reactions at the air−water interface are not. To date, there are no reported studies employing direct measurements of the reaction kinetics at the air−water interface. The goal of this research is aimed to better understand and evaluate the role of interface processes. This work focuses on the development and application of the diffuse reflectance−laser flash photolysis (DR−LFP) technique to study the reactions occurring near the gas−liquid surface. The reaction of $Cl_2^{\bullet-}$ radical anions with ethanol was chosen to directly probe the reaction kinetics close to the air−water interface, because of the appropriate optical properties of that radical.

Accordingly, in this paper we report a diffuse reflectance study of the air−water interface (or close to it) kinetics of the

* To whom correspondence should be addressed. E-mail: Christian.George@univ-lyon1.fr.

[†] Laboratoire d'Application de la Chimie à l'Environnement (UCBL-CNRS).

[‡] Russian Academy of Science.

10.1021/jp026174f CCC: $25.00
Published on Web 03/20/2003

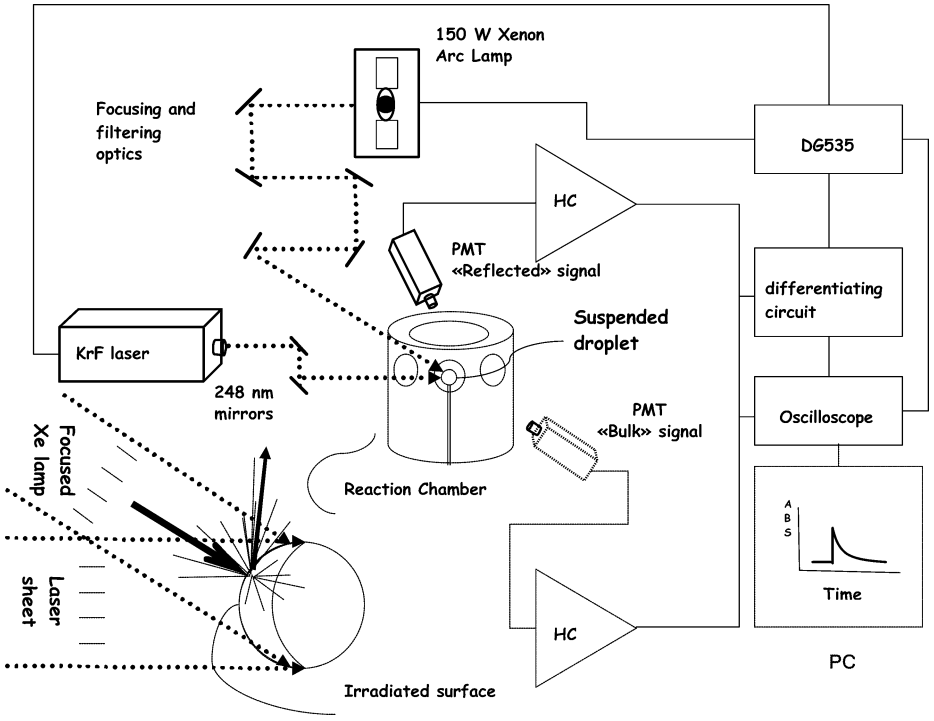

Figure 1. Schematic diagram of the DF−LFP apparatus employed to study the interface kinetics of the $Cl_2^{\bullet-}$ + ethanol reaction. HCA = high-current amplifier, PMT = photomultiplier tube, DG535 = digital delay, and PC = personal computer.

reaction of $Cl_2^{\bullet-}$ radical anions with ethanol. Surface kinetic information is obtained by monitoring absorption of the transient species, i.e.,$Cl_2^{\bullet-}$, following laser flash photolysis of a $K_2S_2O_8$/NaCl/ethanol/H_2O solution. The goal of this research is aimed to better understand and evaluate the role of air−water interface processes of atmospheric interest.

Experimental Section

Methods. The experimental methodology couples radical production by laser flash photolysis (LFP) with time-resolved detection of products using UV diffuse reflectance (DR). A high-pressure xenon arc lamp was used in time-resolved optical absorption by a transient species. The lamp's output wavelength can be filtered to match a specific absorption region of the species of interest. Therefore, the UV DR−LFP technique may be used to monitor concentrations of specific species in solution.

First employed in the 1980s to probe solid heterogeneous systems, the diffuse reflectance−laser flash photolysis technique has become a sensitive tool for understanding the kinetics and mechanisms of photoreactions on many different kinds of solid surfaces and interfaces.[19−24] The diffusion reflectance approach used in this study is similar to one used in previous studies of heterogeneous reactions traditionally performed on solid surfaces (see, for example, refs 5, 19, and 25−27). However, to date, there is no work reported that uses UV diffuse reflectance spectroscopy to directly study reaction kinetics of atmospheric interest at the air−water surface. To our knowledge, this is the first study to use the UV diffuse reflectance time-resolved technique to directly "probe" reaction kinetics on a transparent medium such as a water surface. The UV DR−LFP apparatus used for the $Cl_2^{\bullet-}$ + ethanol experiments is shown schematically in Figure 1. The experiments involve time-resolved detection of $Cl_2^{\bullet-}$ radical anion by optical absorption spectroscopy at $\lambda \approx 350$ nm following 248 nm laser flash photolysis of $K_2S_2O_8$/NaCl/ethanol/H_2O solution according to

$$S_2O_8^{2-} + h\nu\ (\lambda = 248\ \text{nm}) \rightarrow 2SO_4^{\bullet-} \quad (1)$$

$$SO_4^{\bullet-} + Cl^- \rightarrow Cl^{\bullet} + SO_4^{2-} \quad (2)$$

$$Cl\bullet + Cl^- \leftrightarrows Cl_2^{\bullet-} \quad (3)$$

$$Cl_2^{\bullet-} + C_2H_5OH \rightarrow \text{products} \quad (4)$$

$$Cl_2^{\bullet-} + Cl_2^{\bullet-} \rightarrow \text{products} \quad (5)$$

$$Cl_2^{\bullet-} \rightarrow \text{loss} \quad (6)$$

$$Cl^{\bullet} \rightarrow \text{loss} \quad (7)$$

Reaction 2 has been shown to be the rate-determining step in the production of the $Cl_2^{\bullet-}$ radical anion with a reported rate coefficient of $(3.3 \pm 0.5) \times 10^8\ M^{-1}\ s^{-1}$.[28] The reaction of the $Cl^{\bullet}$ radical with ethanol has been omitted from the reaction mechanism above. However, this reaction would not alter the outcome of this study. In reaction mechanism 1−3 the $SO_4^{\bullet-}$ radical anion is converted to $Cl_2^{\bullet-}$ in the presence of Cl^- with a yield of >99.5% in less than 0.2 μs.[29] The decay of $Cl_2^{\bullet-}$ is mapped out on a storage oscilloscope (Tektronix, type 2430A) following a synchronized (under Stanford Research Systems DG535 control) delay between the 248 nm photolysis laser flash and the Xe flash lamp probe pulse. The pulse widths of the 248 nm and Xe flash lamp were 20 ns and 1−11 ms, respectively, while the time scale for the occurrence of the reaction of $Cl_2^{\bullet-}$ with ethanol was typically 0.1−1 ms. All experiments were carried out under strictly pseudo-first-order conditions with Cl^- and ethanol concentrations in excess over the $Cl_2^{\bullet-}$ concentration. Details of the experimental procedure that was employed to study the reaction of $Cl_2^{\bullet-}$ with ethanol are given below.

A cylindrical Teflon reaction cell with an internal volume of ~200 cm^3 was used in all of the $Cl_2^{\bullet-}$ + ethanol experiments.

The internal walls of the reaction vessel were blackened to minimize scattering of radiation. The solution droplet was supported on the flat top of a 6 mm o.d. Teflon tube in the center of the reaction cell. This geometry resulted in a nonspherical droplet of about 8 mm in diameter. Two quartz lenses (focal length 5 cm) and six quartz windows, 2.54 cm o.d., evenly spaced were fixed to the main body of the cell.

The cell was maintained at room temperature. A copper−constantan thermocouple with a stainless steel jacket was inserted into the solution reservoir and the reaction cell through a seal, allowing measurement of the solution and the droplet's surrounding gas medium temperature under the precise experimental conditions employed. The geometry of the reaction vessel was such that it allowed for the photolysis laser and the probe laser beams to enter ∼30° to one another. Two separate photomultiplier tubes were used to monitor the reflected and aqueous-phase, i.e., bulk liquid, signals. One photomultiplier (Hamamatsu H7732-10) was placed at ∼30° relative to the probe beam. The second photomultiplier (Hamamatsu H7826) was positioned on the same axis as the Xe lamp beam. Such detector geometry allowed for the "reflected" and the "bulk" (i.e., transmitted) signals to be collected under the same experimental conditions.

Radiation from a Lambda Physik EMG 101 KrF excimer laser ($\lambda = 248.5$ nm) served as the photolytic light source for the study of the reaction of $Cl_2^{\bullet-}$ radical anions with ethanol. Fluences of 248.5 nm laser radiation utilized in this study were typically 100−130 mJ cm^{-2}, and the laser pulse width was 20 ns. The xenon lamp's output wavelength was filtered to obtain a maximum output radiation at $\lambda \approx 350$ nm to match the maximum absorption region of the $Cl_2^{\bullet-}$ radical anion.[30]

The photolysis laser was triggered at a specific delay time after the probe beam pulse so that the photolysis laser fired in the "plateau" of the Xe flash lamp. Reflected absorption of the $Cl_2^{\bullet-}$ radical anion at $\lambda \approx 350$ nm was collected by a quartz lens on the axis ∼30° to the probe beam, passed through two 350 nm interference filters and a 20% acetonitrile/methanol filter, and imaged onto the photocathode of a photomultiplier tube. The bulk liquid signal was collected on the same axis as the probe beam passing through the droplet using the geometry of lenses and filters as described above.

Given the detector geometry listed above, special care had to be taken so that the reflected signal did not include signal from the bulk-phase processes. That is, the reflected signal may contain information from the bulk-phase processes which result from the internal and diffuse reflections of the analyzing light within the water droplet. As a result, extensive experiments were carried out to ensure that the bulk-phase contribution to the reflected signal was negligible. For example, in one series of preliminary experiments the PMT that measured the reflected signal was placed at various positions around the water droplet. While the observed reflected signal intensity changed, the observed kinetics was always the same. If internal reflections and subsequent transmission of light out of the droplet were significant, then the observed kinetics would have been different at different positions around the water droplet. In another series of preliminary experiments, the excimer laser power and the cross-sectional area of the analyzing light were varied. Similarly, the observed reflected signal intensity varied, but the kinetics remained the same. The maximum intensity of the reflected signal was found to be at an angle of ∼30°. This angle of reflection is consistent with the theoretical work of the reflection−absorption calculations performed by Dluhy.[31] Dluhy's theoretical calculations of the reflection absorption for a monolayer on water suggest that the optical angle for experimental determination of the reflection spectra of thin films on water is in the range 0−40°.[31] Under the experimental conditions employed, assuming a conservative value of 2% reflection[32,33] for the water droplet surface, and using some simple algebra and trigonometry, we can calculate that the reflected signal intensity was at least 10^6 greater than the signal intensity contributed from the bulk-phase processes. However, the reflected signal may still contain information from the bulk-phase processes which result from the fact that the diffuse reflectance−laser flash photolysis technique is not a purely surface specific method. That is, the penetration depth (depth of the solution surface analyzed by the experiment)[32,33] of the analyzing light may be tens of nanometers deep. If the sounding depth is a few tens of nanometers, then there should be a contribution from the bulk phase just below the surface. This point will be discussed later.

Before the photolysis laser was discharged, the "background" steady light level of the Xe lamp was measured by a sample-and-hold circuit using a multimeter. This procedure allowed for the absorption baseline to be obtained. The output pulse from the PMT was passed through a high-speed current amplifier/discriminator (FEMTO HCQ-200M-20K-C), fed to a differentiating circuit that "backed-off" the steady light signal, and then recorded on a storage oscilloscope. The Tektronix storage oscilloscope had a signal-averaging capability and a maximum sampling rate of 100 MHz. The stored signal was digitized and transferred from the oscilloscope to the microcomputer using an IEEE-488 connection. The full absorption signal was then reconstructed from the steady and transient signals. Up to 16 single-shot experiments were averaged to map out a single $Cl_2^{\bullet-}$ radical anion temporal profile over two 1/*e* times.

All experiments were carried out under "static" conditions. However, the solution was allowed to flow using a Watson Marlow 313S liquid pump, and the droplet was replenished after each photolysis laser/flash lamp shot. Therefore, each surface area and volume element of the reaction solution were subjected to only one laser/flash lamp shot, thus preventing the buildup of reaction products on the reaction surface and in the bulk liquid.

Concentrations of each component in the reaction mixture were determined from the appropriate mass and volume measurements. The reaction solution was allowed to flow into the reaction cell from its blackened and foil-coated 1 L storage container. The concentration of $SO_4^{\bullet-}$ in the aqueous phase was not directly measured but was calculated on the basis of experimentally measured and certain known parameters, namely, the quantum yield for $SO_4^{\bullet-}$ radical production from 248 nm photolysis of $S_2O_8^{2-}$, absorption cross section of the $S_2O_8^{2-}$ anion at 248 nm, and laser photon fluence at 248 nm.

Reagents. The reagents used in this work had the following stated minimum purities: $K_2S_2O_8$ (Aldrich, ACS reagent, >99%); NaCl (Aldrich, ACS reagent, >99%; ethanol (Prolabo, absolute, >99.8%). All solutions were prepared using water with a resistivity of >18 MΩ cm. Deionized water was prepared by passing tap water through a reverse osmosis demineralization filter (ATS Groupe Osmose) followed by a commercial deionizer (Millipore, Milli-Q[50]). All solutions were used within 1 h of their preparation. All experiments were performed with a pH value of ∼5.8. A possible impurity in $K_2S_2O_8$ was sulfuric acid. However, if potassium persulfate was predominantly responsible for controlling the pH of our solutions, then a pH of 5.8 would be equivalent to a sulfuric acid content of ∼0.003%.

Results and Discussions

Adding ethanol to water modifies the surface tension of the surface. As a result, the concentration profile near the surface is altered. The concentration of ethanol at the water droplet surface, $[\text{ethanol}]^{\sigma}$, was estimated on the basis of the work of Donaldson and co-workers[12,34−36] and Strey and co-workers[37] using a Langmuir-type isotherm:

$$[\text{ethanol}]^{\sigma} \equiv \Gamma = \frac{\Gamma_{\text{sat}}[\text{ethanol}]_{\text{bulk}}}{b + [\text{ethanol}]_{\text{bulk}}} \quad \text{(I)}$$

In eq I, Γ and Γ_{sat} are the surface coverage and saturated surface coverage, respectively, and the parameter b is related to the rate coefficients for adsorption and desorption from the surface into the liquid bulk. It should be noted that eq I adopted from the work of Donaldson and co-workers[12,34−36] and Strey and co-workers[37] is an approximation. The left side of eq I, Γ, is not really the surface coverage (concentration) of ethanol but relative adsorption of ethanol with respect to water. However, for low concentrations of bulk ethanol, and assuming monolayer segregation, the surface excess and surface concentrations are approximately the same.

The concentration of ethanol at the interface, $[\text{ethanol}]^{\sigma}$, was calculated using Gibbs approach[38] where the relative surface excess of species i was expressed as

$$\Gamma_{\text{H2O},i} = \left(\frac{\partial\sigma}{\partial\mu_i}\right)_{T,\mu j\neq 1} = \left(-\frac{a_i}{RT}\right)\left(\frac{\partial\sigma}{\partial a_i}\right) \quad \text{(II)}$$

for adsorption from the bulk liquid.[34] In eq II $\Gamma_{\text{H2O},i}$ is the surface coverage of species i, σ is the surface tension, μ_i is the chemical potential of species i, a_i is the activity of species i, R is the gas constant, and T is the absolute temperature. (Hereinafter, $\Gamma_{\text{H2O},i}$ will be abbreviated to Γ.) Here, similar to the work of Donaldson and Anderson on adsorption of C_1–C_4 alcohols, acids, and acetone gases at the air−water interface, solution concentrations were used rather than activities.[34] The use of solution concentrations is consistent with the work of Strey and co-workers on the necessity of using activities in the Gibbs equation.[37] Equilibrium surface tensions of aqueous ethanol solutions were taken from the work of Strey and co-workers.[37] On the basis of the work of Donaldson and Anderson, the following exponential polynomial function was used to fit surface tension data:[34]

$$\sigma = \sigma_0 e^{-a1[\text{ethanol}]} + a_2[\text{ethanol}] + a_3[\text{ethanol}]^2 + a_4[\text{ethanol}]^3 \quad \text{(III)}$$

In eq III, [ethanol] is the aqueous-phase ethanol concentration (mol L^{-1}) and σ_0 is the surface tension of pure water (σ_0 = 72.0 dyn cm^{-1}). The derivative of eq III was then used to calculate the relative surface excess via the Gibbs equation:[34]

$$\frac{d}{d[\text{ethanol}]}(\sigma) = -\sigma_0 a_1 e^{-a1[\text{ethanol}]} + a_2 + 2a_3[\text{ethanol}] + 3a_4[\text{ethanol}]^2 \quad \text{(IV)}$$

The saturated surface coverage, Γ_{sat}, was then obtained from least-squares analysis to a Langmuir isotherm. The Γ_{sat} and b are found to be 3×10^{13} molecules cm^{-2} and 0.3, respectively. Once Γ_{sat}, the parameter b, and the bulk ethanol concentration were known, the "real" surface ethanol concentration, Γ, was calculated.

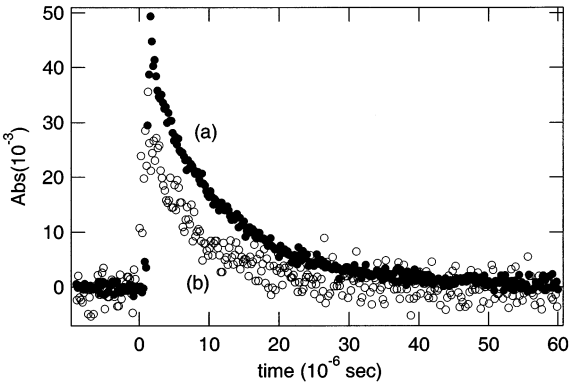

Figure 2. Typical (a) bulk and (b) surface $Cl_2^{\bullet-}$ absorbance temporal profiles observed in the study of the reaction of $Cl_2^{\bullet-}$ with ethanol. The photolysis laser was fired at time 0. Experimental conditions: T = 298 K; [NaCl] = 50 mM; $[K_2S_2O_8]$ = 5 mM; [ethanol] = 0.3 M. The number of laser shots averaged was 16.

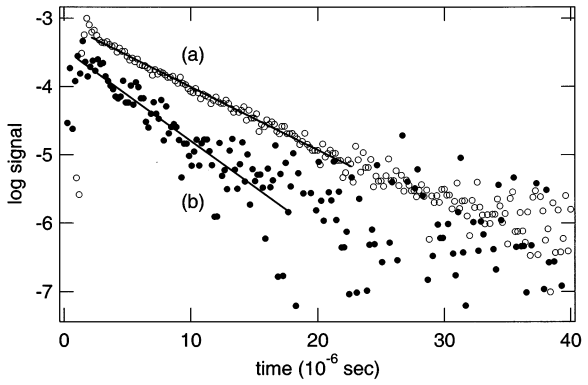

Figure 3. Typical (a) bulk and (b) surface $Cl_2^{\bullet-}$ first-order decays observed in the study of the $Cl_2^{\bullet-}$ + ethanol reaction. The photolysis laser was fired at time 0. Experimental conditions: T = 298 K; [NaCl] = 50 mM; $[K_2S_2O_8]$ = 5 mM; [ethanol] = 0.3 M. The number of laser shots averaged was 16. Fits are obtained from linear least-squares analyses and give the following first-order decays (10^3 s^{-1}): (a) 87, (b) 120.

All experiments were carried out under pseudo-first-order conditions with Cl^- and ethanol concentrations in excess over the $Cl_2^{\bullet-}$ radical anion concentration. Typical liquid bulk Cl^- and $S_2O_8^{2-}$ concentrations were 50 and 5 mM, respectively, while aqueous-phase ethanol concentrations were in the range from 0.11 to 0.64 M. Some typical surface and bulk liquid $Cl_2^{\bullet-}$ radical anion temporal profiles observed following laser flash photolysis of $K_2S_2O_8$/NaCl/ethanol/water mixtures are shown in Figure 2. Typical first-order plots for the "surface" and bulk channels are shown in Figures 3 and 4. The bimolecular plots for the reaction of $Cl_2^{\bullet-}$ with ethanol are shown in Figure 5. The effective surface and bulk liquid rate coefficients, k_{obsd}(surface) and k_{obsd}(bulk), respectively, are obtained from the variation of the corresponding pseudo-first-order rate coefficient, k' (for the bulk) and k'^{σ} (for the surface), with [ethanol] at constant concentrations of Cl^- and $S_2O_8^{2-}$. The plot of the pseudo-first-order rate coefficient k'^{σ} versus the ethanol surface concentration from which the rate coefficient for the surface reaction of the $Cl_2^{\bullet-}$ anion with ethanol was extracted is shown in Figure 6. The observed surface rate coefficient for the reaction of the $Cl_2^{\bullet-}$ radical anion with ethanol is found to be strictly proportional to the ethanol surface concentration (see Figure 6). Fits to plots of k_{obsd}(surface) and k_{obsd}(bulk) vs [ethanol] in the aqueous phase are described by the following expressions:

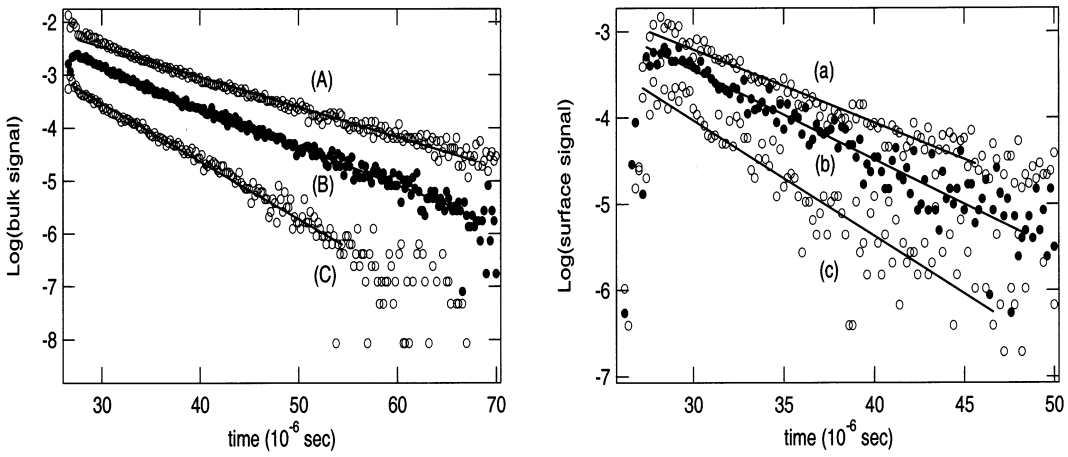

Figure 4. Typical $Cl_2^{\bullet-}$ first-order temporal profiles observed for the (A−C) bulk and a−c surface in the study of the reaction of $Cl_2^{\bullet-}$ with ethanol. The photolysis laser was fired at time 0. Experimental conditions: $T = 298$ K; [NaCl] = 50 mM; [$K_2S_2O_8$] = 5 mM. [Ethanol] (M): (A, a) 0.08, (B, b) 0.15, (C, c) 0.3. The number of laser shots averaged was 16. Solid lines are obtained from least-squares analyses that give the following best-fit k' parameters (10^3 s^{-1}): (A) 55, (B) 74, (C) 110, (a) 77, (b) 104, (c) 160.

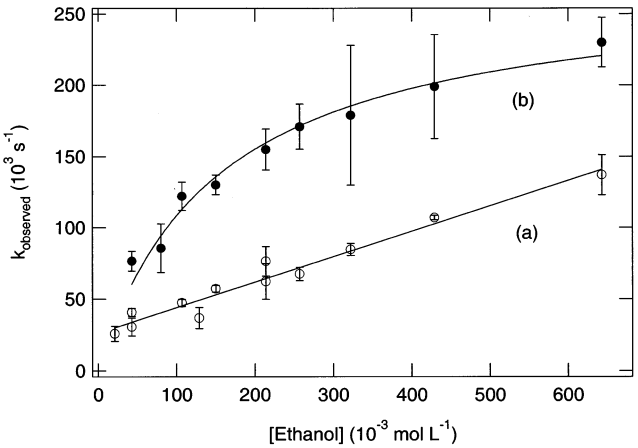

Figure 5. k' versus [ethanol] for (a) bulk and (b) surface data obtained in the studies of the reaction of $Cl_2^{\bullet-}$ with ethanol. Fits are obtained from a linear least-squares analysis and Langmuir equation and give the following bimolecular rate coefficients (10^5 M^{-1} s^{-1}): (a) 1.77 ± 0.34 and (b) 4.45 ± 0.80, respectively. Uncertainties are 2σ and represent precision only.

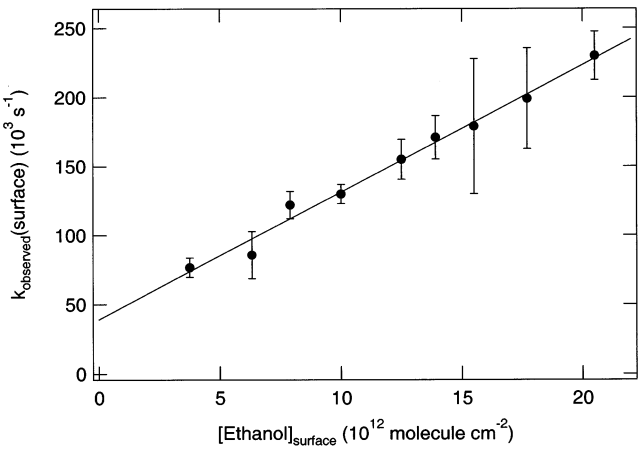

Figure 6. Pseudo-first-order rate coefficient k'^{σ} versus ethanol surface concentration from which the rate coefficient for the surface reaction of the $Cl_2^{\bullet-}$ anion with ethanol was extracted. The fit is obtained from a linear least-squares analysis and results in a bimolecular rate coefficient equal to (9.22 ± 0.82) × 10^{-9} cm^2 s^{-1} $molecule^{-1}$ for an arbitrary penetration depth of 0.8 nm. Uncertainties are 2σ and represent precision only.

$$k_{obsd}(\text{surface}) = k'^{\sigma}[\text{ethanol}]^{\sigma} + k_0{}^{\sigma} \qquad \text{(V)}$$

$$k_{obsd}(\text{bulk}) = k'[\text{ethanol}] + k_0 \qquad \text{(VI)}$$

In eqs V and VI, k'^{σ} and k' are the second-order rate coefficients for the decay of $Cl_2^{\bullet-}$ at the surface and in the aqueous phase, respectively, [ethanol]$^{\sigma}$ and [ethanol] are ethanol concentrations at the surface and in the bulk liquid, respectively, and $k_0{}^{\sigma}$ and k_0 are surface and bulk, respectively, pseudo-first-order rate coefficients for the $Cl_2^{\bullet-}$ decay in the absence of ethanol. It should be noted in Figure 5 that the kinetics at the surface do not increase linearly with the bulk liquid ethanol concentration. It is observed that the nonlinear behavior of the experimental kinetic data for the surface shows a Langmuir-type dependence on concentration. Therefore, the data presented in Figures 5 and 6 indicate that the reaction $Cl_2^{\bullet-}$ + ethanol at the air−water surface can be described by a dynamic Langmuir model. Accordingly, since the kinetics at the interface are consistent with a Langmuir-type description, we report with confidence that we are, indeed, observing the diffuse reflectance signal originating at the surface (or just beneath it) and not in the bulk liquid. Also, it should be noted that the deviation from the first-order behavior of the decay of the $Cl_2^{\bullet-}$ radical anion may arise as a result of the fast self-recombination of $Cl_2^{\bullet-}$ anions (i.e., reaction 3). The rate coefficients for reaction 3 have been reported to be (1.8 ± 0.1) × 10^9 M^{-1} s^{-1} [29] at $I \rightarrow 0$ (I = ionic strength) and $T = 298$ K and 7 × 10^8 M^{-1} s^{-1}.[39] Under the experimental conditions employed in this work we estimate a "first-order" contribution from reaction 3 to be <200 s^{-1} to the measured first-order rate coefficient for the reaction of $Cl_2^{\bullet-}$ with ethanol. Indeed, as shown in Figures 3 and 4 the decay profiles of the $Cl_2^{\bullet-}$ concentration were always observed to follow first-order kinetics. Therefore, the nonlinear behavior of our surface signal (as shown in Figure 5) can be safely attributed to surface processes.

The following surface and aqueous-phase rate coefficients for the reaction of $Cl_2^{\bullet-}$ with ethanol are derived from the data:

$$k_{obsd}(\text{surface}) = (9.22 \pm 0.82) \times 10^{-9}\ \text{cm}^2\ \text{s}^{-1}\ \text{molecule}^{-1} \qquad \text{(VIII)}$$

$$k_{obsd}(\text{bulk}) = (1.77 \pm 0.34) \times 10^5\ \text{M}^{-1}\ \text{s}^{-1} \qquad \text{(IX)}$$

Assuming arbitrarily the interface depth of 0.8 nm, k_{obsd}(surface) $= (4.45 \pm 0.80) \times 10^5$ M^{-1} s^{-1}. Uncertainties in the above equations are 2σ and represent precision only (all data points weighted equally). The only other direct measurements of the effective rate coefficient for the reaction of $Cl_2^{\bullet-}$ + ethanol in the aqueous phase were carried out by Zellner and co-workers,[29] Hasegawa and Neta,[40] and Khmelinskii et al.[41] We find that the observed rate coefficient for the reaction of $Cl_2^{\bullet-}$ with ethanol in the aqueous phase agrees well within the error limits with the recent work by Zellner and co-workers, $(1.2 \pm 0.2) \times 10^5$ M^{-1} s^{-1}.[29] However, Hasegawa and Neta and Khmelinskii et al. report rate coefficients for the aqueous-phase reaction of $Cl_2^{\bullet-}$ with ethanol to be $(4.5 \pm 0.9) \times 10^4$ and 1.4×10^4 M^{-1} s^{-1}, respectively. These studies were performed at moderate to high ionic strengths. While the work of Hasegawa and Neta was carried out at an ionic strength $I = 1$ M, the study by Khmelinskii et al. was carried out in the presence of 10.3 M HCl. It has been shown that increasing ionic strength can decrease the rate constant for H-atom abstraction reactions of $Cl_2^{\bullet-}$.[29] The higher ionic strength may result in ion pairing in concentrated aqueous salt solutions.[42] As a result, the lower rate coefficients reported by Hasegawa and Neta and Khmelinskii et al. may be the result of ion pairing between the $Cl_2^{\bullet-}$ radical anions and the Na^+ cations since the $NaCl_2$ complex might have a reduced reactivity compared to the free $Cl_2^{\bullet-}$ radical anion.[29] The experimental conditions of Jacobi et al. were similar to the experimental conditions employed in this study. Therefore, we report with confidence that our result for the effective rate coefficient for the aqueous-phase reaction of $Cl_2^{\bullet-}$ with ethanol to be consistent with the work by Zellner and co-workers.

On the other hand, we find that the effective rate coefficient for the reaction of $Cl_2^{\bullet-}$ with ethanol at the air−water surface is estimated to be about a factor of 2 higher than the experimental value in the bulk liquid. There are no other kinetic data for the reaction of $Cl_2^{\bullet-}$ with ethanol at the air−water interface reported in the literature with which to compare our results.

Since the diffuse reflectance−laser flash photolysis technique is not a purely surface sensitive method, the real value of the enhancement in reactivity at the surface cannot be firmly established since we did not know the effective sounding depth of the experiment. If we crudely estimate a sounding depth of $\lambda/4$, then we are probing a depth of about 90 nm. As a result, the contribution from the bulk-phase processes cannot be excluded. Unfortunately, our current experimental setup does not allow us to quantify the contribution from the bulk-phase processes resulting from the penetration depth of the analyzing light. We are currently working on this problem.

However, on the basis of the kinetics and the Langmuir-type adsorption of ethanol at the water surface, we believe that the observed reflectance signal must originate near the surface. In principle, our sounding depth may range from a few angstroms (i.e., the lower limit of the air−water interface thickness) to few tens of nanometers (at the upper end of the concentration profile of ethanol due to the Gibbs surface excess). As this depth is used to convert our surface kinetics to standard units of M^{-1} s^{-1} (for comparison purposes) and because our kinetics are integrated all over that depth, we cannot provide a real enhancement factor but only provide a safe lower limit of about a factor of 2.

Nevertheless, the observed enhanced reactivity at the air−water phase boundary may be explained in terms of physical processes at the water droplet surface. For instance, traditionally, water−vapor interfaces were described as regions of continuous variation of density[43] caused by density fluctuations within the liquid bulk phases.[44−46] Later studies[47,48] assumed a steplike local density profile across the liquid−gas interface, whose width is the result of the propagation of thermally excited capillary waves.[49] It is however clear that the interface is a region where the density decreases sharply from its bulk water value to the one of the gas phase. This density lowering is accompanied by a potential increase of the mobility of "solutes" at the interface, which in turn may affect the surface reaction by increasing the frequency of encounters between molecules. To react, hydrated molecules have to move through a dense medium (i.e., water in our case) and displace H_2O molecules from their solvation shells before leading to reaction encounters. All these processes cost energy to the system, which may slow the overall kinetics. At the surface, the situation may be somehow different (and slightly closer to the gas phase, where such solvation shells mostly do not exist). In fact, the solvation of a molecule at the surface may not be complete (i.e., the number of H_2O molecules close to a given species may be much lower than in the bulk), which in turn may affect any potential kinetics, and the thermodynamics playing a role in the chemical transformation may be altered (a lower energy cost may be followed by a faster reaction). Another aspect that may change the surface kinetics of chloride-containing solutions is the structure-breaking feature of that anion illustrated by a slightly increased Cl^- concentration (compared to its bulk value) just below the surface of the air−water interface.[50] This is a property which is introduced by the solvation thermodynamics of the anion. Associated with the Gibbs excess of ethanol, this additional Cl^- excess may be the source of the reactivity enhancement. However, this structure-breaking nature of the chloride anion has only been illustrated in water (and only in small clusters and lamellae) and not in water/ethanol mixtures. We believe that, in the latter case, it is the ethanol properties that govern the surface tension of the droplet and, therefore, the surface composition, repelling from the surface any Cl^- excess. The latter if it exists may then be below the ethanol excess (a sandwich-like surface), which then may not affect the surface kinetics. If Cl^- anions are squeezed from the surface, then we would have deviation from the Langmuir isotherm. This is not observed. On the other hand, our kinetics are first order and, therefore, not dependent on the $Cl_2^{\bullet-}$ radical anion concentration. Accordingly, we believe that we have indeed observed an enhanced reactivity for the surface reaction of the $Cl_2^{\bullet-}$ radical anion with ethanol.

An important assumption in this work is that the kinetics of the reaction of the $Cl_2^{\bullet-}$ radical anion with ethanol can be separated into the surface and bulk processes. However, on the time scale of the experiment ($\sim$10 μs), the reactants can diffuse distances on the order of a hundred nanometers. Therefore, any enhanced rate at the surface will influence the concentrations to a depth of around half a wavelength of the analyzing light. Consequently, a full kinetic model of the reflectivity has to include mass transport as well as chemical reaction. If we assume that the $Cl_2^{\bullet-}$ radical anion decays at the same rate both at the surface and in the bulk and that at the time of flash photolysis we have a homogeneous system (i.e., $[Cl_2^{\bullet-}]_{surface} = [Cl_2^{\bullet-}]_{bulk}$), then no concentration gradient will exist between the surface and the bulk phase. As a result, surface kinetics will not be influenced by the bulk-phase processes. On the other hand, if we assume that the concentrations of the $Cl_2^{\bullet-}$ radical anion both at the surface and in the bulk are the same but the corresponding rate of the $Cl_2^{\bullet-}$ radical anion decay at the surface is faster than in the bulk, then surface kinetics will be influenced by the bulk-phase processes due to the diffusion from the bulk

toward the surface. This will result in a lower observed rate coefficient for the surface reaction of the $Cl_2^{\bullet-}$ radical anion with ethanol. If this is the case, the rate coefficient presented here for the surface reaction of the $Cl_2^{\bullet-}$ radical anion with ethanol (eq VIII) should be considered a lower limit. If the reaction at the surface is slower than in the bulk liquid, then the $Cl_2^{\bullet-}$ radical anion may diffuse from the surface to the bulk. In this case, the surface rate coefficient would be described by the bulk-phase kinetics and the measured surface rate coefficient will be the upper limit for the bulk phase reaction of the $Cl_2^{\bullet-}$ radical anion with ethanol.

Conclusions

In summary, we have successfully applied the UV DR−LFP technique to directly study the reaction kinetics at the air−water phase boundary. The reaction of the $Cl_2^{\bullet-}$ radical anion with ethanol was chosen to directly probe the reaction kinetics at the air−water surface. Results presented here for the reaction of $Cl_2^{\bullet-}$ with ethanol in the aqueous phase agree well with the literature value. On the other hand, results presented here for the surface reaction of the $Cl_2^{\bullet-}$ radical anion with ethanol indicate a reactivity enhancement at the air−water surface. The observed rate coefficient for the reaction of $Cl_2^{\bullet-}$ with ethanol at the air−water phase boundary is found to be at least a factor of 2 higher than the experimental value in the bulk liquid. Therefore, the rate coefficient for the surface reaction of the $Cl_2^{\bullet-}$ radical anion with ethanol presented here (eq VIII) should be considered a lower limit on the basis of the uncertainties in mass exchange and sounding depth of the experiment.

The particular measurements made here may not have direct atmospheric implications, as $Cl_2^{\bullet-}$ is not a major oxidizer under typical atmospheric conditions (maybe except in the marine environment where the Cl^- content of sea salt aerosols may be large enough to produce $Cl_2^{\bullet-}$ in sufficient amounts to become a radical of atmospheric importance). However, the higher effective rate coefficient for the surface reaction $Cl_2^{\bullet-}$ + ethanol obtained in this study, if proved to be a general feature and therefore extended to a wider range of compounds, could have important atmospheric implications for model calculations of other relevant tropospheric and stratospheric heterogeneous reactions on liquid surfaces. In fact, aerosols are by nature very dispersed. For example, under typical midlatitude stratospheric conditions, 15−25 km altitude, the size of aerosols is in the range 0.1−1 μm and the surface area is in the range 10^{-9}−10^{-8} cm^2/cm^3.[51] The temperature in this region of the atmosphere ranges from 215 to 220 K, and the aerosol is expected to be a supercooled liquid.[52] Tropospheric clouds are composed of droplets ranging in size from 5 to 50 μm and have a corresponding liquid surface area on the order of 10^{-3} cm^2/cm^3.[2] Since the global average cloud volume is about 15%,[2] clouds provide a substantial reactive surface area for heterogeneous reactions. The surface-to-volume ratio of a liquid droplet can be very simply calculated to be $3/r$ (where r is the radius), which underlines the fact that, for small droplets (such as those encountered in a typical aerosol or even fog or clouds), the ratio starts to be in favor of the surface. This illustrates (in an extremely simple way) that any surface process has the potential to become important. Therefore, we believe that enhanced reactivity at the air−water interface may have important implications on the reactivity of certain atmospheric environments which need to be proved by forthcoming experiments not only on the kinetics but also on the mechanistic changes at the interface.

Clearly, in addition to this study, further research and more investigations of the reaction kinetics at the air−water surface are warranted. Further experiments of atmospheric importance on the direct measurement of diffuse reflectance signals at the air−water phase boundary are in progress.

Acknowledgment. We gratefully acknowledge the support of the French Atmospheric Chemistry Program PNCA for this work. We thank Dr. Colin D. Bain at the University of Oxford, U.K., for helpful discussions.

References and Notes

(1) Charlson, R. J.; Langer, J.; Rodhe, H. *Nature* **1990**, *348*, 22.
(2) Lelieveld, J.; Crutzen, P. J. *Nature* **1990**, *343*, 6225.
(3) Solomon, S. *Rev. Geophys.* **1988**, *26*, 131.
(4) Davidovits, P.; Hu, J. H.; Worsnop, D. R.; Zahnister, M. S.; Kolb, C. E. *Faraday Discuss.* **1995**, *100*, 65.
(5) Finlayson-Pitts, B. J.; Pitts, J. N. *Chemistry of the Upper and Lower Atmosphere: Theory, Experiments and Applications*; Academic Press: San Diego, 2000.
(6) Magi, L.; Schweitzer, F.; Pallares, C.; Cherif, S.; Mirabel, P.; George, C. *J. Phys. Chem. A* **1997**, *101*, 4943.
(7) DeMore, W. B.; Sander, S. P.; Golden, D. M.; Hampson, R. F.; Kurylo, M. J.; Howard, C. J.; Ravishankara, A. R.; Kolb, C. E.; Molina, M. J. *Chemical Kinetics and Photochemical Data for Use in Stratospheric Modeling*; Pasadena, California, 1997.
(8) Fockenberg, C.; Saathoff, H.; Zellner, R. *Chem. Phys. Lett.* **1994**, *218*, 21.
(9) Spicer, C. W.; Chapman, E. G.; Finlayson-Pitts, B. J.; Plastridge, R. A.; Hubbe, J. M.; Fast, J. D.; Berkowitz, C. M. *Nature* **1998**, *394*, 353.
(10) Knipping, E. M.; Lakin, M. J.; Foster, K. L.; Jungwirth, P.; Tobias, D. J.; Gerber, R. B.; Dabdub, D.; Finlayson-Pitts, B. J. *Science* **2000**, *288*, 301.
(11) Jayne, J. T.; Davidovits, P.; Worsnop, D. R.; Zahnister, M. S.; Kolb, C. E. *J. Phys. Chem.* **1990**, *94*, 6041.
(12) Donaldson, D. J.; Guest, J. A.; Goh, M. C. *J. Phys. Chem.* **1995**, *99*, 9313.
(13) Jayne, J. T.; Duan, S. X.; Davidovits, P.; Worsnop, D. R.; Zahnister, M. S.; Kolb, C. E. *J. Phys. Chem.* **1992**, *96*, 5452.
(14) Schweitzer, F.; Magi, L.; Mirabel, P.; George, C. *J. Phys. Chem. A* **1998**, *102*, 593.
(15) Hu, J. H.; Shi, Q.; Davidovits, P.; Worsnop, D. R.; Zahnister, M. S.; Kolb, C. E. *J. Phys. Chem.* **1995**, *99*, 8768.
(16) Hanson, D. R. *J. Phys. Chem. B* **1997**, *101*, 4998.
(17) Katrib, Y.; Deiber, G.; Schweitzer, F.; Mirabel, P.; George, C. *Aerosol Sci.* **2001**, *32*, 893.
(18) George, C.; Behnke, W.; Scheer, V.; Zetzsch, C.; Magi, L.; Ponche, J. L.; Mirabel, P. *Geophys. Res. Lett.* **1995**, *22*, 1505.
(19) Wilkinson, F. *J. Chem. Soc., Faraday Trans. 2* **1986**, *82*, 2073.
(20) Shen, Y. R. *IEEE J. Sel. Top. Quantum Electron.* **2000**, *6*, 1375.
(21) Shen, Y. R. *Nature* **1989**, *337*, 519.
(22) Wilkinson, F.; Willsher, C. J.; Leicester, P. A.; Barr, J. R. M.; Smith, M. J. C. *J. Chem. Soc., Chem. Commun.* **1986**, 1216.
(23) Miragliotta, J. A. *Johns Hopkins APL Tech. Dig.* **1995**, *16*, 348.
(24) Borensztein, Y. *Surf. Rev. Lett.* **2000**, *7*, 399.
(25) Vogt, R.; Finlayson-Pitts, B. J. *J. Phys. Chem.* **1995**, *99*, 13052.
(26) Vogt, R.; Finlayson-Pitts, B. J. *J. Phys. Chem.* **1994**, *98*, 3747.
(27) Langer, S.; Pemberton, R. S.; Finlayson-Pitts, B. J. *J. Phys. Chem. A* **1997**, *101*, 1277.
(28) Herrmann, H.; Jacobi, H.-W.; Reese, A.; Zellner, R. *Proceedings of EUROTRAC Symposium '96*; Computational Mechanics Publications: Southampton, U.K., 1997; Vol. 1.
(29) Jacobi, H.-W.; Wicktor, F.; Herrmann, H.; Zellner, R. *Int. J. Chem. Kinet.* **1999**, *31*, 169.
(30) Herrmann, H. Photochemische Bildung, Spektroskopie und Kinetik freier Radikale in wässerige Lösung. Habilitation Thesis, Universität GH Essen, Essen, Germany, 1997.
(31) Dluhy, R. A. *J. Phys. Chem.* **1986**, *90*, 1373.
(32) Harrick, N. J. *Internal Reflection Spectroscopy*; Interscience Publishers: New York, 1967.
(33) Kortüm, G. *Reflectance spectroscopy. Principles, methods, applications*; Springer: Berlin, Heidelberg, New York, 1969.
(34) Donaldson, D. J.; Anderson, D. *J. Phys. Chem. A* **1999**, *103*, 871.
(35) Donaldson, D. J. *J. Phys. Chem. A* **1999**, *103*, 62.
(36) Demou, E.; Donaldson, D. J. *J. Phys. Chem. A* **2002**, *106*, 982.
(37) Strey, R.; Viisanen, Y.; Aratono, M.; Kratohvil, J. P.; Yin, Q.; Friberg, S. E. *J. Phys. Chem. B* **1999**, *103*, 9112.
(38) Adamson, A. W. **1990**.
(39) McElroy, W. J. *J. Phys. Chem.* **1990**, *94*, 2435.
(40) Hasegawa, K.; Neta, P. *J. Phys. Chem.* **1978**, *82*, 854.
(41) Khmelinskii, I. V.; Plyusnin, V. F.; Grivin, V. P. R. *J. Phys. Chem.* **1989**, *63*, 2722.

(42) Perlmutter-Hayman, B. *J. Phys. Chem. Ref. Data* **1981**, *10*, 671.
(43) Waals, J. D. v. d. *Verh. K. Akad. Wet. Amsterdam* **1893**, 1.
(44) Rowlinson, J. S.; Widom, B. *Molecular Theory of Capillarity*; Oxford University Press: Oxford, 1982.
(45) Cahn, J. W.; Hilliard, J. E. *J. Chem. Phys.* **1958**, *28*, 258.
(46) Fisk, S.; Widom, B. *J. Chem. Phys.* **1960**, *50*, 3219.
(47) Buff, F. P.; Lovett, R. A.; Stillinger, R. H. *Phys. Rev. Lett.* **1965**, *15*, 621.
(48) Gelfand, M. P.; Fisher, M. E. *Physica A* **1990**, *166*, 1.
(49) Fradin, C.; Braslau, A.; Luzet, D.; Smilgies, D.; Alba, M.; Boudet, N.; Mecke, K.; Daillant, J. *Nature* **2000**, *403*, 871.
(50) Stuart, S. J.; Berne, B. J. *J. Phys. Chem. A* **1999**, *103*, 10300.
(51) Turco, R. P.; Toon, O. B.; Hamill, P. *J. Geophys. Res.* **1989**, *94*, 16493.
(52) Steele, H. M.; Hamill, P.; McCormick, M. P.; Swissler, T. J. *J. Atmos. Sci.* **1983**, *40*, 2055.